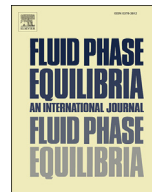




Contents lists available at ScienceDirect

Fluid Phase Equilibria

journal homepage: www.elsevier.com/locate/fluid

Phase behavior and solid–liquid equilibria of aliphatic and aromatic carboxylic acid mixtures

Kazuhiro Tamura^{*}, Tsuyoshi Kasuga, Tomoyuki Nakagawa

Faculty of Natural System, Institute of Science and Engineering, Kanazawa University, Kakuma-machi, Kanazawa, 920-1192, Japan

ARTICLE INFO

Article history:

Received 29 September 2015

Received in revised form

7 December 2015

Accepted 10 December 2015

Available online xxx

Keywords:

Peritectic system

Eutectic system

Solid–liquid equilibria

Phase equilibrium calculation

ABSTRACT

We newly developed an apparatus for the solid–liquid equilibrium measurements to examine the phase equilibria of carboxylic acid mixtures. The equilibrium freezing temperatures obtained from the cooling curve of the liquid state to solid were measured for the stearic acid + benzoic acid, adipic acid + benzoic acid, and *p*-toluic acid + benzoic acid systems. The experimental results were correlated successfully by Wilson, NRTL, and UNIQUAC models. Moreover thermodynamic approach of Slaughter and Doherty was applied to represent the solid–liquid equilibria of peritectic and eutectic compound exists in the solid phase due to the reaction of complex formation. Good agreement between the experimental and calculated values for the binary carboxylic acid mixtures was obtained.

© 2015 Elsevier B.V. All rights reserved.

1. Introduction

Pharmaceutical, cosmetic, and food industries make good use of fatty acids and their mixture as addition ingredients to the products. The fatty acid mixtures act as a surface and viscosity modifier and stabilizer additive by adjusting fusion characteristics in accordance with the melting temperature of fatty acids. The phase behavior and transition phenomena of fatty acid mixtures have been examined intensively by differential scanning calorimetry (DSC) and complemented by different types of X-ray, NMR, and IR and FT-Raman spectroscopy analyses [1,2]. It was revealed that the phase diagram for the fatty acid mixtures is quite complicated and exhibits eutectic and peritectic points, where a new solid compound forms in solid phase due to the difference in the molecular interactions between like and unlike molecules. Besides fatty acid and their methyl ester as major components in biodiesel fuel made from natural vegetable oils attracts a current interest in renewable energy sources as energy alternatives of fossil fuel. In the upstream and downstream processing, it is important to understand the phase behavior of mixtures containing fatty acids. So the precise and reliable phase equilibrium data are necessary for a proper design of the refinery process as well as for a further development of thermodynamic predictive models. Solid–liquid equilibrium

measurements have been carried out using several different kinds of techniques [3–8]; analytical, synthetic, and visual methods, dynamic determination of melting and cooling curves, and pour/cloud test.

In the present work we newly made an apparatus for solid–liquid equilibrium measurements to examine the phase equilibria of carboxylic acid mixtures. The apparatus consists of heating and cooling systems for the measurements of equilibrium temperature and light scattering intensity measurement system that can detect a change from liquid mixture to solid-state formation. The light scattering intensity measurement was secondarily performed to observe the solid formation. We aim to study the phase and solid–liquid equilibria for aliphatic and aromatic carboxylic acid mixtures. The equilibrium freezing temperatures and eutectic and peritectic points for stearic acid + benzoic acid, adipic acid + benzoic acid, and *p*-toluic acid + benzoic acid mixtures were measured from the cooling temperature profiles of the liquid state to solid. The experimental results of the binary mixtures were correlated by the Wilson [9], NRTL [10], and UNIQUAC [11] models. Moreover the experimental data were examined by comparing with those calculated from the thermodynamic approach [12–14] for a peritectic and eutectic compound exists in the solid phase due to the reaction of complex formation.

2. Experimental

Adipic acid, and benzoic acid, and naphthalene were purchased

^{*} Corresponding author.

E-mail address: tamura@se.kanazawa-u.ac.jp (K. Tamura).

from Wako Chemicals, stearic acid and p-toluic acid were from Tokyo Chemical Industry, and phenanthrene from Sigma–Aldrich Co. The purity and melting point of the chemicals were given in Table 1. The melting temperatures of the materials were in good agreement with literature [1,15–18] and they were used without further purification.

A schematic diagram of the calorimeter is illustrated in Fig. 1 (a). The apparatus was designed for the determination of equilibrium freezing and eutectic points from the cooling temperature curve. Additionally the measuring system equipped a laser light source with a light detector to observe the solid-state formation from the change of light scattering intensity, as shown in Fig. 1 (b). The apparatus consists of an equilibrium cell with the capacity about 8 cm³. Solidus binary sample prepared gravimetrically at a specified composition was loaded in the cell and heated to melt above a higher melting temperature of every pure component. The resultant liquid sample mixture was homogenized by stirring with a magnetic stirrer vigorously. Then the melting mixture was cooled to 303.15 K at a cooling rate of 1.0 K/min. The rate of temperature change in the vicinity of the phase transition was controlled within 0.1 K/min by data acquisition and control system (Keyence, KV-300, KVTP40). The temperature in the cell was measured every second by a platinum temperature-sensing probe within ± 0.01 K. The equilibrium temperature was obtained from the cooling curve of the liquid state to solid as well as the derivative of the temperature with respect to time. Fig. 2 depicts practical exemplification in determination of the freezing temperature from the cooling temperature profiles of pure component and binary mixtures. The measurements were triplicated to ensure reproducibility in the determination of equilibrium liquid temperature. The experimental uncertainties in the temperature were estimated as not larger than 0.5 K.

The experimental setup was validated by comparing the freezing temperature measured for naphthalene and phenanthrene mixture with the literature [19]. Table 2 lists the experimental data for the naphthalene and phenanthrene system measured in this work. Fig. 3 shows the freezing temperature of naphthalene and phenanthrene mixture was in good agreement with the literature values within average temperature deviation of 1.5 K. Table 3 summarized the experimental freezing temperatures (T_L) and eutectic temperatures (T_E) in the solid–liquid equilibria for the carboxylic acid mixtures. As shown in Fig. 4, it was found that the stearic acid + benzoic acid, adipic acid + benzoic acid, and p-toluic acid + benzoic acid systems exhibited the eutectic and peritectic points in phase behavior. Besides the freezing temperatures of the adipic acid + benzoic acid mixture at the mole fraction range of adipic acid up to 0.2 was lower than those of Wang et al. [16] obtained from the differential scanning calorimetry (DSC) and a peritectic point of the stearic acid + benzoic acid system appears

Table 1
Purity of chemicals used and melting temperatures.

Compound	Purity, mass fraction	T_m /K	
		This work	Literature
Adipic acid	>0.995	426.35	425.65 ^a , 426.31 ^b , 426.35 ^c
Benzoic acid	>0.995	395.50	395.50 ^a , 396.08 ^b
Naphthalene	>0.98	353.41	352.41 ^a , 353.4 ^d
Phenanthrene	>0.98	372.39	372.39 ^a , 372.4 ^d
Stearic acid	>0.98	342.95	342.45 ^a , 342.95 ^e
p-toluic acid	>0.98	452.75	452.75 ^{a,c}

^a [15].

^b [16].

^c [17].

^d [18].

^e [1].

around the adipic acid mole fraction of 0.2 was observed in this work.

3. Calculated results

The experimental results were analyzed by thermodynamic framework of solid–liquid equilibria [20]. The thermodynamic criteria of solid–liquid equilibria is described by

$$\ln(z_i \gamma_i^S / x_i \gamma_i^L) = \frac{\Delta H_i}{RT_{m,i}} \left(\frac{T_{m,i}}{T} - 1 \right) \quad (1)$$

where z_i and x_i are the mole fraction of component i in solid and liquid phases, γ_i^S and γ_i^L the activity coefficients in solid and liquid phases, $\Delta_{fus}H_i$ the enthalpy of fusion, $T_{m,i}$ the melting temperature. For the system with the pure immiscible solids exist in the solid phase, as known eutectic solid mixture, the term $z_i \gamma_i^S$ in Eq. (1) equals to unity. The equilibrium liquidus temperature of the mixture can be expressed by

$$T = \Delta_{fus}H_i / \left[\frac{\Delta_{fus}H_i}{T_{m,i}} - R \ln(x_i \gamma_i^L) \right] \quad (2)$$

The experimental results measured in the present work were correlated using the Wilson model [9], NRTL model ($\alpha_{ij} = 0.3$) [10], and UNIQUAC model [11]. Table 4 lists the physical properties of carboxylic acids and the UNIQUAC volume and surface parameters estimated by the group contribution method of Fredenslund et al. [21]. The binary interaction parameters in the activity coefficient models were obtained fitting the model to the experimental data by minimizing the objective function:

$$F = \sum_{i=1}^N \left(\frac{T_{exp,i} - T_{calc,i}}{T_{exp,i}} \right)^2 \quad (3)$$

The absolute arithmetic mean deviation AAD was defined by

$$AAD = 100 \sum_{i=1}^N \frac{|T_{exp,i} - T_{calc,i}|}{T_{exp,i}} / N \quad (4)$$

where N is the number of experimental data. The binary energy parameters ($\lambda_{ji} - \lambda_{ii}$), ($g_{ji} - g_{ii}$), ($u_{ji} - u_{ii}$) in the Wilson model, NRTL model ($\alpha_{ij} = 0.3$), and UNIQUAC model were determined as fitting parameters by a numerical iterative procedure available from Refs. [10,20]. Table 5 presents the binary parameters along with the absolute arithmetic mean deviation AAD between the experimental and calculated values. Compared with the UNIQUAC model, the Wilson and NRTL models exhibited the higher AAD of 1% in reproducing the freezing temperatures for the stearic acid + benzoic acid system. As can be seen in Fig. 5, a peritectic point of the stearic acid + benzoic acid system appears around the mole fraction of stearic acid, 0.6 and an inflection on the freezing temperature curve were observed. As the same reported previously for fatty acid mixtures in the solid phase [1,2], this phase behavior could be related to the formation of peritectic compound and phase transition. The peritectic solid mixture is the system that perfectly miscible solids exist in the solid phase to form a new solid compound due to the molecular interactions between unlike molecules.

In the representation for the peritectic system, Slauter and Doherty [12] suggested the chemical reaction between pure solid components A and B in the solid phase. The equilibrium constant K was defined by the activity of chemical species as

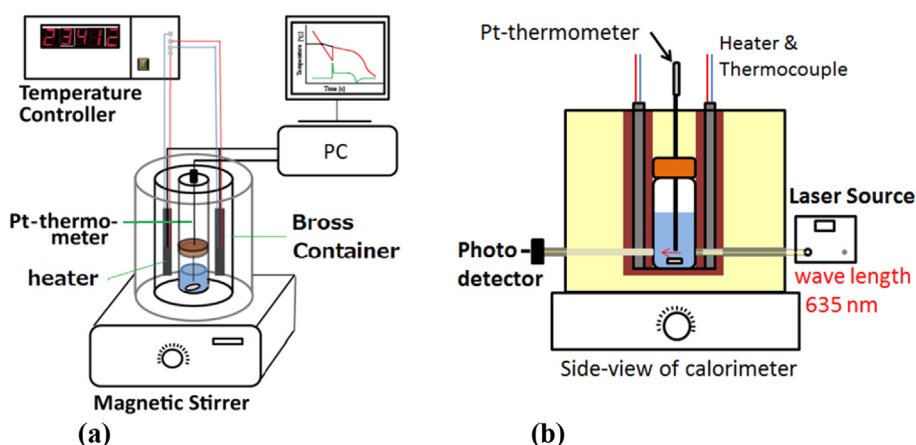


Fig. 1. (a) Experimental setup (b) Light scattering intensity measurement.

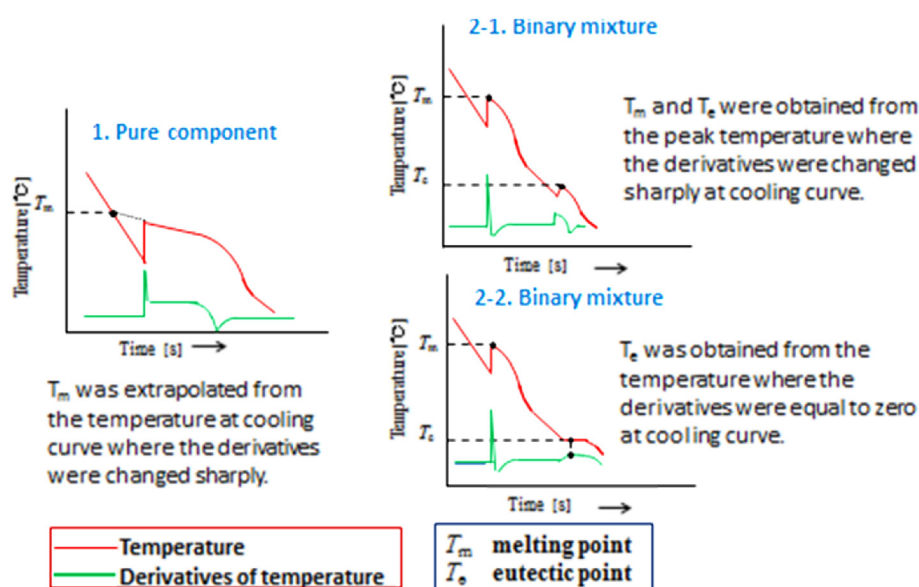


Fig. 2. Typical temperature profiles at cooling condition and determination of freezing and eutectic points from the cooling curve.

$$K = \prod_{i=A} (z_i \gamma_i^S)^{\nu_i} = \exp\left(\frac{-\Delta G_R^0}{RT}\right) = \exp\left(-\frac{\Delta H_R^0}{RT} + \frac{\Delta S_R^0}{R}\right) \quad (5)$$

where $\Delta G_R^0 (= \Delta H_R^0 - T\Delta S_R^0)$ is the standard Gibbs energy change of reaction, ΔH_R^0 and ΔS_R^0 the enthalpy and entropy change of reaction and ν_i the stoichiometric coefficient of component i in the reaction: $|\nu_1|A + |\nu_2|B = \nu_3C$. Based on the thermodynamic modeling scheme of Slauter and Doherty [12], Rocha and Guirardello [14] proposed a new approach to determine the freezing temperature of solid–liquid equilibria by using the minimization of the Gibbs energy of

Table 2
Experimental SLE data for naphthalene (1) + phenanthrene (2) system.

x_1	T_L/K	T_E/K	x_1	T_L/K	T_E/K
0.0000	370.32		0.6000	324.18	322.62
0.1000	362.58	318.55	0.7000	332.48	323.12
0.2000	355.22	320.75	0.8000	339.22	323.02
0.3000	346.25	321.35	0.9000	346.42	322.75
0.4000	336.35	322.25	1.0000	351.98	
0.5000	326.02	322.55			

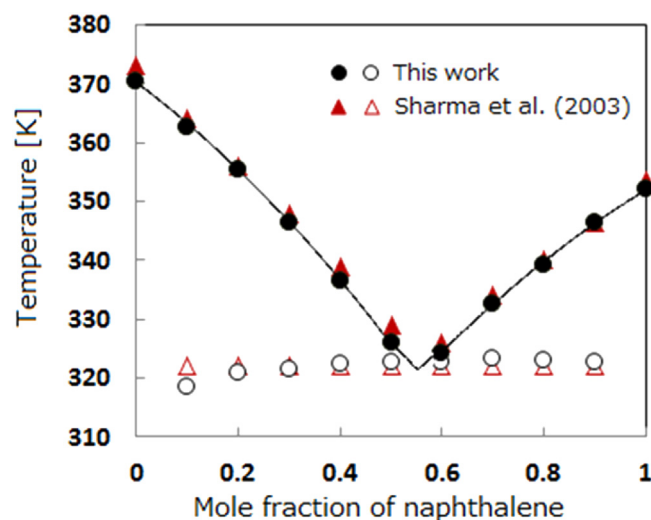


Fig. 3. Comparison of experimental solid–liquid equilibria for naphthalene + phenanthrene system with literature and calculated values. (●, ○), Experimental; (▲, △), Sharma et al. (2003). (—), calculated by Wilson model with binary parameters given in Table 5.

Table 3
Experimental SLE data for binary systems.

x_1	p-toluic acid (1) + benzoic acid (2)		Adipic acid (1) + benzoic acid (2)		Stearic acid (1) + benzoic acid (2)	
	T_L/K	T_E/K	T_L/K	T_E/K	T_L/K	T_E/K
0.0000	396.28		396.28		396.28	
0.0500			387.88	375.25		
0.1000	383.25	364.45	384.12	376.08	384.35	333.90
0.1500			377.98	375.48		
0.2000	371.55	364.20	378.08	375.15	371.48	333.88
0.2250	369.65	364.35				
0.2500	369.85	365.05	378.08	377.82		
0.2800	368.85	368.85				
0.3000	370.20	369.75	381.62	377.95	360.25	333.75
0.3500	381.75	370.55				
0.4000	389.90	369.35	392.95	377.15	346.40	334.25
0.5000	403.10	369.15	399.98	377.48	343.35	334.08
0.6000	416.25	368.05	406.05	377.52	333.88	333.12
0.7000	426.40	365.00	410.82	376.85	335.78	331.15
0.8000	436.30	361.50	415.68	376.58	338.18	329.65
0.9000	443.95	361.10	420.75	374.65	340.12	327.85
1.0000	451.60		425.58		341.78	

the mixture. The total Gibbs energy of the mixtures G can be given by the sum of the Gibbs energy in solid and liquid phases and of reaction as follows:

$$G = RT(z_A \ln z_A \gamma_A^S + z_B \ln z_B \gamma_B^S) + RT(x_A \ln \gamma_A^L x_A + x_B \ln \gamma_B^L x_B) + x_A(\mu_A^{OL} - \mu_A^{OS}) + x_B(\mu_B^{OL} - \mu_B^{OS}) + \Delta G_R^0 \quad (6)$$

where $(\mu_i^{OL} - \mu_i^{OS})$ is the difference of pure component chemical potential in liquid and solid phases, which can be determined from Eq. (1). Consider the complex formation occurs only in solid phase, $z_A \gamma_A^S = z_B \gamma_B^S = 1$ for the miscible solid phase. Following the

calculation procedure [14] to minimize the Gibbs energy of the mixture given by Eq. (6), the equilibrium freezing temperature of the mixture can be expressed analytically in following three regions;

Region (1),

$$T = \Delta_{fus} H_2 / \left[\frac{\Delta_{fus} H_2}{T_{m,2}} - R \ln(x_B \gamma_B^L) \right] \quad (7)$$

with the restriction obtained from the intersection of equilibrium curves of Eqs. (7) and (11),

$$\left[\frac{\Delta_{fus} H_1}{RT_{m,1}} \left(\frac{T_{m,1}}{T} - 1 \right) + \ln(x_A \gamma_A^L) \right] \leq \frac{\Delta G_R^0}{\nu_1 RT} \quad (8)$$

Region (2),

$$T = \Delta_{fus} H_1 / \left[\frac{\Delta_{fus} H_1}{T_{m,1}} - R \ln(x_A \gamma_A^L) \right] \quad (9)$$

with the restriction from the intersection of equilibrium curves of Eqs. (9) and (11),

$$\left[\frac{\Delta_{fus} H_2}{RT_{m,2}} \left(\frac{T_{m,2}}{T} - 1 \right) + \ln(x_B \gamma_B^L) \right] \leq \frac{\Delta G_R^0}{\nu_2 RT} \quad (10)$$

Region (3),

$$T = \left[\nu_1 |\Delta_{fus} H_1 + \nu_2 |\Delta_{fus} H_2 - \Delta G_R^0 \right] / \left[\frac{\nu_1 |\Delta_{fus} H_1}{T_{m,1}} + \frac{\nu_2 |\Delta_{fus} H_2}{T_{m,2}} - \nu_1 |R \ln(x_A \gamma_A^L) - \nu_2 |R \ln(x_B \gamma_B^L) \right] \quad (11)$$

with the restriction obtained from Eqs. (8) and (10),

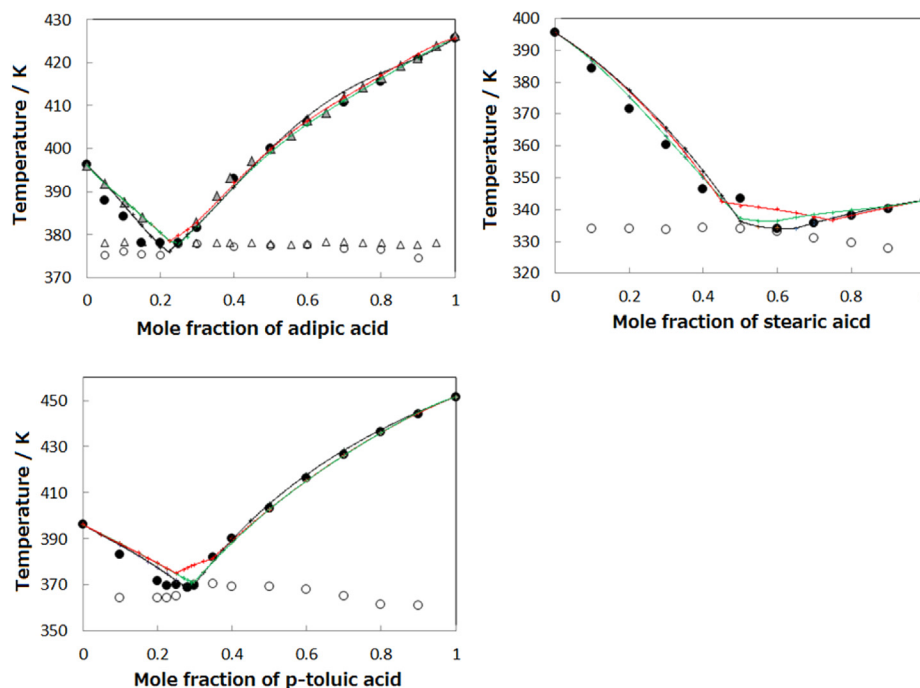


Fig. 4. Solid–liquid equilibria for three systems of binary acid mixtures. (—), calculated by one-suffix Margules equation with ΔG_R^0 as adjustable parameter, (—), calculated by one-suffix Margules equation with ΔH_R^0 and ΔS_R^0 as adjustable parameters, and (—), two-suffix Margules equation with ΔG_R^0 as adjustable parameter. Experimental (\bullet , \circ), this work, (\blacktriangle , \triangle), Wang et al. (2010).

Table 4

Melting temperature, enthalpy of fusion, and UNIQUAC volume and surface structural parameters.

Compound	$T_{m,i}/K$	$\Delta_{fus}H_i/kJ\ mol^{-1}$	r_i	q_i
Adipic acid ^a	426.35	34.85	5.3002	4.608
Benzoic acid ^b	395.50	18.02	4.3230	3.344
Naphthalene ^c	353.41	18.70	4.9808	3.440
Phenanthrene ^c	372.39	16.46	6.7738	4.480
Stearic acid ^d	342.95	59.50	12.9928	10.712
p-toluic acid ^b	452.75	22.70	5.0580	3.912

^a [17].^b [15].^c [18].^d [1].

$$\frac{\Delta G_R^0}{|\nu_1|RT} \leq \left[\frac{\Delta_{fus}H_1}{RT_{m,1}} \left(\frac{T_{m,1}}{T} - 1 \right) + \ln(x_A \gamma_A^L) \right] \leq 0, \quad (12)$$

$$\frac{\Delta G_R^0}{|\nu_2|RT} \leq \left[\frac{\Delta_{fus}H_2}{RT_{m,2}} \left(\frac{T_{m,2}}{T} - 1 \right) + \ln(x_B \gamma_B^L) \right] \leq 0$$

Table 5

Correlated results for binary systems by Wilson, NRTL, and UNIQUAC models.

System (1 + 2)	Wilson		NRTL ^a		UNIQUAC	
	$(\lambda_{12}-\lambda_{11})/R/K$ $(\lambda_{21}-\lambda_{22})/R/K$	AAD/%	$(g_{12}-g_{22})/R/K$ $(g_{21}-g_{11})/R/K$	AAD/%	$(u_{12}-u_{22})/R/K$ $(u_{21}-u_{11})/R/K$	AAD/%
Naphthalene + phenanthrene	-145.60 195.22	0.07	-349.80 431.40	0.10	-132.90 150.64	0.08
Adipic acid + benzoic acid	-222.46 317.98	0.52	418.93 -280.46	0.52	270.15 -200.58	0.53
Stearic acid + benzoic acid	-676.24 503.02	1.22	-490.88 502.58	1.18	644.82 -297.98	0.84
p-toluic acid + benzoic acid	247.00 -243.92	0.62	785.85 -530.78	0.70	354.07 -256.35	0.68

^a Nonrandomness factor, α_{ij} , in NRTL model was set to 0.3.

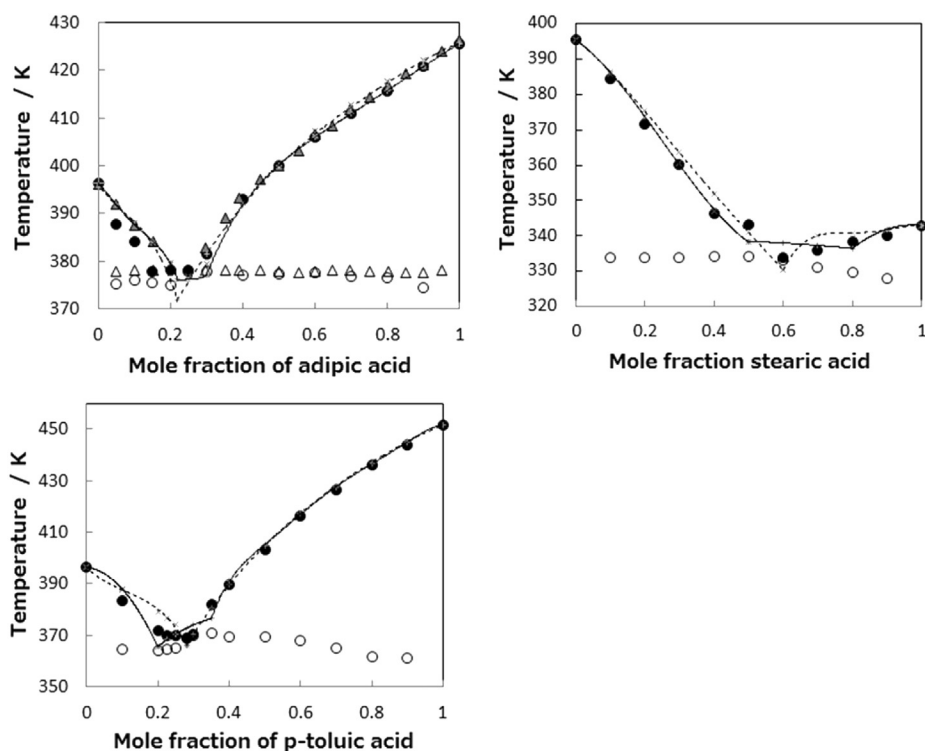


Fig. 5. Solid–liquid equilibria for three systems of binary acid mixtures. (—), calculated by UNIQUAC model with ΔG_R^0 as adjustable parameter, and (---), calculated by UNIQUAC model alone. Experimental (●, ○), this work, (▲, △), Wang et al. (2010).

The two-suffix Margules equation for liquid phase activity coefficient was firstly applied to calculate the solid–liquid equilibria.

$$RT \ln \gamma_A^L = [A_{12} + 2(A_{21} - A_{12})x_A]x_B^2, \quad (13)$$

$$RT \ln \gamma_B^L = [A_{21} + 2(A_{12} - A_{21})x_B]x_A^2$$

We assumed the AB complex formation ($|\nu_1| = |\nu_2| = 1$) between pure acids A and B in the solid phase in accordance with the chemical reaction $A + B = AB$ at the first. The binary parameters A_{21} and A_{12} in Eq. (13) and standard Gibbs energy of reaction ΔG_R^0 in Eqs. (8), (10) and (12) were determined by minimizing the objective function of Eq. (3). Table 6 summarizes the AAD obtained in fitting the model to the experimental results measured in the present work, where ΔG_R^0 , ΔH_R^0 and ΔS_R^0 as adjustable parameters as well as binary parameters A_{12} and A_{21} in the Margules equation were regressed in three parts; (a) Margules one-suffix with constant ΔG_R^0 , (b) Margules two-suffix with constant ΔG_R^0 , and (c) Margules one-suffix with constant ΔH_R^0 and ΔS_R^0 (so that ΔG_R^0 varies with temperature). Increasing the number of fitting parameters in the regression decreased the AAD for three binary mixtures, but

Table 6
Correlated results for binary systems by Margules equation with ΔG_R^0 , ΔH_R^0 , and ΔS_R^0 .

System (A + B)	A_{12} /J mol ⁻¹	A_{21} /J mol ⁻¹	ΔG_{R0} /J mol ⁻¹	ΔH_{R0} /J mol ⁻¹	ΔS_{R0} /J mol ⁻¹ K ⁻¹	AAD/%
Adipic acid + benzoic acid	-526.70		-453.21			0.47
	-1899.83	955.14	-1073.14			0.44
	-501.60			2062.48	6.14707	0.47
Stearic acid + benzoic acid	3303.72		-1184.53			0.86
	-2846.08	1411.32	-528.53			0.81
	3500.00			4914.20	23.0963	0.83
p-toluic acid + benzoic acid	787.46		-891.04			0.88
	1997.50	-202.76	-228.06			0.54
	771.81			1264.10	3.6959	0.69

Table 7
Correlated results for binary systems by UNIQUAC model with ΔG_R^0 .

System (A + B)	$(u_{12}-u_{22})/R$ /K $(u_{21}-u_{11})/R$ /K	$\Delta G_{R0}/J$ mol ⁻¹	AAD/%
Adipic acid + benzoic acid	316.49	-313.45	0.56
	-224.20		
	311.08 ^a -222.79 ^a	-992.1 ^a	0.52 ^a
Stearic acid + benzoic acid	667.57	-1398.23	0.56
	-314.23		
p-toluic acid + benzoic acid	244.15	-1461.87	0.63
	-194.30		

^a AB₂ complex formation between adipic acid and benzoic acid was assumed additionally.

worked negatively in the representation of the eutectic and peritectic points as shown in Fig. 4. Secondly we applied the UNIQUAC model for liquid phase activity coefficient to calculate the solid–liquid equilibria with the AB complex formation ($|\nu_1| = |\nu_2| = 1$) between pure acids A and B in the solid phase. Table 7 summarizes the AAD and the binary parameter in the UNIQUAC model and standard Gibbs energy of reaction obtained in fitting the model to the experimental results measured in the present work. The correlated results for the stearic acid + benzoic system were improved significantly in comparison with those obtained by the Wilson and NRTL models alone with the parameters given in Table 5. Fig. 5 shows the calculated results for the binary carboxylic acid mixtures taking into account chemical equilibria in the solid phase agreed well with the experimental ones in comparison with those calculated by the UNIQUAC model alone. Additionally we assumed AB₂ complex formation ($|\nu_1| = 1, |\nu_2| = 2$) in addition to AB complex for the adipic acid + benzoic acid system due to the fact that adipic acid includes two COOH groups in a molecule capable of forming the complex of AB and AB₂. Setting the same value of ΔG_R^0 for the AB and AB₂ complex formation made a slight improvement in the representation of the eutectic and peritectic system for the adipic acid + benzoic acid system as shown in Table 7.

4. Conclusion

We newly developed an apparatus for the solid–liquid equilibrium measurements to investigate the phase equilibria of carboxylic acid mixtures. The freezing and eutectic temperatures were

determined from the cooling curves. The solid–liquid equilibrium data for binary mixtures of adipic acid + benzoic acid, stearic acid + benzoic acid, and p-toluic acid + benzoic acid systems were presented and shows the eutectic and peritectic points. The experimental results were able to correlate by the Wilson, NRTL, and UNIQUAC models. Moreover the solid–liquid equilibria for the peritectic systems were represented successfully by the thermodynamic model with complex formation between unlike molecules in the solid phase. For the adipic acid + benzoic acid mixture, AB₂ complex formation between adipic acid and benzoic acid made a slight improvement in the representation of the eutectic and peritectic system. It was found that the thermodynamic representation considering chemical equilibria in the solid phase can give accuracy improvement to the solid–liquid equilibria and eutectic and peritectic points for binary acid mixtures studied in the present work.

References

- [1] T. Inoue, Y. Hisatsugu, R. Yamamoto, M. Suzuki, Chem. Phys. Lipids 127 (2004) 143–152.
- [2] M.C. Costa, M. Sardo, M.P. Rolemberg, P.R. Claro, A.J.A. Meirelles, J.A.P. Coutinho, M.A. Krähenbühl, Chem. Phys. Lipids 157 (2009) 40–50.
- [3] J. Lohmann, R. Joh, J. Gmehling, J. Chem. Eng. Data 42 (1997) 1170–1175.
- [4] A. Jakob, R. Joh, C. Rose, J. Gmehling, Fluid Phase Equilib. 113 (1995) 117–126.
- [5] H. Matsuda, H. Kimura, Y. Nagano, K. Kurihara, K. Tochigi, K. Ochi, J. Chem. Eng. Data 56 (2011) 1500–1505.
- [6] J.B. Ott, J.R. Goates, A.H. Budge, J. Phys. Chem. 66 (1962) 1387–1390.
- [7] M. Tadie, I. Bahadur, P. Reddy, P.T. Ngema, P. Naidoo, N. Deenadayalu, D. Ramjugernath, J. Chem. Thermodyn. 57 (2013) 485–492.
- [8] H. Imahara, E. Minami, S. Saka, Fuel 85 (2006) 1666–1670.
- [9] G.M. Wilson, J. Am. Chem. Soc. 86 (1964) 127–130.
- [10] H. Renon, J.M. Prausnitz, A.I.Ch.E. J. 14 (1968) 135–144.
- [11] J.M. Prausnitz, R.N. Lichtenthaler, E.G.A. Azevedo, Molecular Thermodynamics of Fluid-phase Equilibria, Prentice-Hall, N. Y., 1999.
- [12] D.W. Slaughter, M. Doherty, Chem. Eng. Sci. 50 (1995) 1679–1694.
- [13] M.C. Costa, M.P. Rolemberg, L.A.D. Boros, M.A. Krähenbühl, M.G. de Oliveira, A.J.A. Meirelles, J. Chem. Eng. Data 52 (2007) 30–36.
- [14] S.A. Rocha, R. Guirardello, Fluid Phase Equilib. 281 (2009) 12–21.
- [15] W.M. Haynes, CRC Handbook of Chemistry and Physics, 95th ed., CRC Press, 2014–2015.
- [16] T.-C. Wang, T.-Y. Lai, Y.-P. Chen, J. Chem. Eng. Data 55 (2010) 5797–5800.
- [17] A. Cingolani, G. Berchiesi, J. Therm. Anal. 6 (1974) 87–90.
- [18] M.V. Roux, M. Temprado, J.S. Chickos, Y. Nagano, J. Phys. Chem. Ref. Data 37 (2008) 1855–1996.
- [19] B.L. Sharma, R. Kant, R. Sharma, S. Tandon, Mater. Chem. Phys. 82 (2003) 216–224.
- [20] S.I. Sandler, Chemical, Biochemical, and Engineering Thermodynamics, fourth ed., John Wiley & Sons, Inc., U.S.A., 2006.
- [21] A. Fredenslund, J. Gmehling, P. Rasmussen, Vapor-liquid Equilibria Using UNIFAC, Elsevier, Amsterdam, 1977.